Journal of Nuclear Materials 103 & 104 (1981) 427-432
North-Holland Publishing Company

THE STRUCTURE OF GRAPHITE AND SILICON CARBIDE RESULTING FROM HELIUM-ION BOMBARDMENT

D.J. Bacon, I. Dümler and A.S. Rao*

Department of Metallurgy and Materials Science,
The University, P.O. Box 147, Liverpool L69 3BX, England.

(* Now in: Physics Division, Argonne National Laboratory, Illinois)

Graphite and silicon carbide have been irradiated with helium ions, and, in addition to surface changes, microstructural effects have been studied using transmission-electron microscopy. Ion energies and doses up to 100 keV and 5 x 10^{18} cm^{-2}, respectively, have been employed for specimen temperatures in the range 20°-700°C. Graphite crystals are found to deform by twinning, and the density of twins can be correlated to the dimensional changes expected in irradiated graphite. Blistering is only found in very thin films. Silicon carbide exhibits a gas-driven flaking at high temperatures, but at 20°C does not flake. This difference is shown to be related to a temperature-dependence of structural changes produced by the ions.

1. INTRODUCTION

The harsh irradiation environment materials are likely to encounter in the vicinity of the plasma in operational fusion power reactors has already set in train extensive research into the effects of ion bombardment on the structure of metals. This is necessary, not only to aid in future materials selection, but also to provide a fundamental understanding of the atomic form and evolution of defects in damaged crystals. Experiments involving heavy- and light-ion beams are required to simulate the effects of 14 MeV neutrons and 3.5 MeV alpha particles and gases produced by transmutation reactions. Although there is as yet a lack of understanding of the factors controlling radiation-induced dislocation structure in many metals, the effects of light, gas-ion bombardment are well-documented(1,2); blistering and erosion of the surface ensue from gas-bubble formation at a depth related to the ion concentration/dpa versus depth profiles. The situation in ceramic materials is less clear-cut, and this is unfortunate for they are likely to find application in a number of situations where the radiation flux is high(3).

The confused picture is typified by graphite, long considered a possible shielding material, for which investigators have reported conflicting effects under helium or hydrogen beams ranging from blistering to crazing, and from twinning to cracking: for reviews see(4). A similar variety of effects has been reported for other ceramics. In silicon carbide, for example, bombardment with deuterium or helium ions has been observed(5,6,7) to produce surface roughening, resulting possibly from blistering, in contrast to a report(8) of no change in surface topography; a conclusion(9) that under similar conditions the surface is depleted of carbon is at variance with evidence from Raman spectroscopy that it becomes carbon-rich, as well as amorphous(5).

Most of the observations have relied on the scanning electron microscope (sem), yet clearly much of the detail of the ion damage requires investigation of the sub-surface microstructure. We have therefore used the transmission electron microscope (tem) to study the effects of helium-ion damage on graphite and silicon carbide. The results and their interpretation are reported in the following two sections.

2. GRAPHITE

2.1 Procedure and Results

The graphite samples were prepared from either natural, single crystals or highly-oriented pyrolytic graphite; the latter material was produced by the Union Carbide Corp. and has a high degree of crystal perfection. The natural crystals were examined optically before and after bombardment, and thin flakes were cleaved from the injected surface for examination in the tem as required. Samples from the hopg material were prethinned (to approximately 0.1 μm) by cleavage so that they could be examined in the tem before and after ion irradiation. $^4He^+$ ions of energy 70 or 100 keV, flux in the range 1-5x10^{14} $cm^{-2}s^{-1}$ and dose up to 10^{18} cm^{-2} were injected in the HIA at Harwell. Target temperatures between 20° and 700°C were used, and the surface normal was [0001].

Full details of the observations are reported elsewhere(4), but in summary two important effects were found. In samples of thickness ≥ 0.1 μm, ion irradiation induces the graphite to twin. The twins are clearly revealed by optical examination of unthinned samples, as shown by the example in fig.1, and are seen in the tem in specimens cleaved from such samples and in the thicker prethinned hopg specimens.

0022-3115/81/0000–0000/$02.75

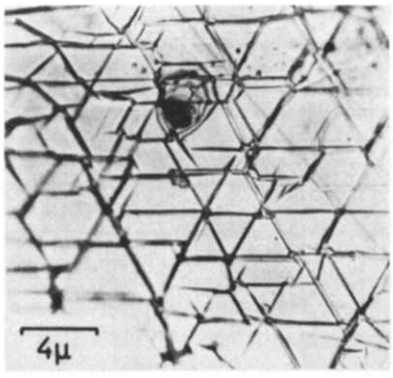

Figure 1: Optical micrograph of natural crystal irradiated with 100 keV ions at 20°C to a dose of 10^{18} cm^{-2}.

The crystallography of the twins was determined by electron-diffraction analysis, and the majority had habit planes and shear directions of either $\{11\bar{2}\bar{1}\}$ $\langle 11\bar{2}6\rangle$ or $\{10\bar{1}1\}$ $\langle 10\bar{1}2\rangle$. The density of twinned crystal was measured from the area fraction of twins on the injected surface; an example is given by the 'experimental' data in fig. 2. The density decreases

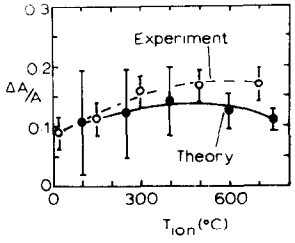

Figure 2: Twin density for thick samples injected with 100 keV ions to a dose of 10^{18} cm^{-2}.

as the energy and dose are decreased(4), and the fraction of twinned material is insignificant for doses $\lesssim 10^{16}$ cm^{-2}.

From examination of the prethinned hopg material, it was found that the twin density reduces to zero as the sample thickness falls below about 0.05 μm, and for specimen temperatures below about 300°C, no ion-induced effects are seen. For temperatures $\gtrsim$300°C, and particularly in the thicker tem samples, curved domes reminiscent of blisters are produced by the ion bombardment: a typical observation is reproduced in fig. 3. The domes have mean diameter between 1 μm and 4.3 μm, being smallest at 300°C, and, from measurements on their bend contours, have heights of only a few tens of nm. In addition to the domes, contrast consistent with small (∿2-20 nm) clusters of interstitials is seen in samples irradiated at 500° and 700°C.

A few samples were injected with 100 keV deuterons at either 20° or 500°C, and the effects

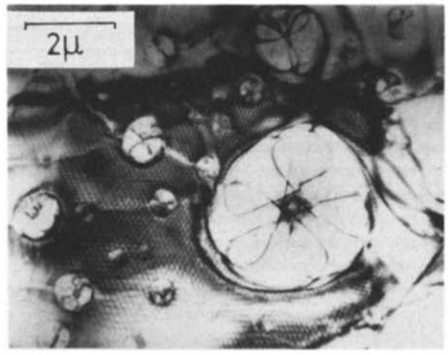

Figure 3: Tem image of thinned sample injected with 100 keV ions at 500°C to a dose of 10^{18} cm^{-2}.

produced were very similar to those seen after helium injection, but in crystals bombarded with carbon ions, only twinning and contrast from small interstitial clusters were found. Twins have also been found in single crystals by Mazey and Barnes(10) after irradiation with a variety of ion species. It is clear, therefore, that twinning is the main structural effect produced by ion irradiation and is not specifically associated with light, gaseous ions.

2.2 Discussion

Twinning is the one deformation mode in graphite that gives rise to shear strains acting out of the basal plane. It is probable, therefore, that it occurred here to relieve the build-up of stress which results from displacement damage produced by the ions. For 100 keV ions of dose 10^{18} cm^{-2}, this damage builds up from a surface value just above 3 dpa to a peak of about 24 dpa at a depth close to 0.5 μm. The damage is associated with lattice parameter and dimensional changes in the graphite, and although these properties have not been measured for ion irradiation, data for neutron-irradiated graphite are in the literature. Details of how the data can be converted to the damage rates realized with ions are given elsewhere(4).

The twin density required to accommodate normal strains e_a and e_c parallel and perpendicular to the basal plane, respectively, is found to be 0.93 $(e_c - e_a)$, irrespective of the twin mode involved(4). For the sample orientation employed in the present work, e_c produces a uniform lifting of the surface and can be ignored: e_a has a strong dependence on dpa value and temperature, and by taking the difference between its value at 0.5 μm and the surface, the theoretical curve of fig. 2 is obtained: the bars reflect the uncertainty that arises from extrapolating the neutron data. The agreement between theory and experiment is considered to

be adequate for confirmation of the model in which twinning accommodates the (differential) dimensional changes produced by displacement damage. This model is also consistent with the reduction in twin density observed when lower ion energies and doses are employed, and it predicts the absence of twinning in very thin crystals.

It has been shown(4) that the shallow blisters seen in prethinned tem flakes can be produced by very small quantities of gas, i.e. << dose. The mechanism by which these blisters form is not known and it is not understood why they are not seen on the surface of bulk samples. One possibility is that the low cleavage stress of graphite enables blisters to spread laterally, so that the domes have low curvature and are not easily detectable. Interestingly, the surface does bulge upwards between the twins for irradiation temperatures $\gtrsim 300^{\circ}C$(4), but it seems unlikely that this is due to a gas-driven distortion for it also occurs after irradiation with carbon ions: it may arise after the onset of twinning from the [0001] component of strain (e_c).

Examination of reports in the literature of gas-ion-induced surface changes in graphite suggests that no unambiguous identification of blistering has been made. Many of the experiments have been carried out on pyrolytic and other polycrystalline graphites of more complicated structure than the crystals used here. It is very likely, therefore, that the 'wrinkling', 'crazing', 'surface raising' and blistering' reported elsewhere are manifestations of the dimensional changes and twinning produced in the individual crystallites. The sink for the injected gas, of which about 7-10% is retained (4), is still unknown, however, and further study is required.

3. SILICON CARBIDE

3.1 Procedure and Results

The material selected for study was 'Refel', a reacton-bonded, polycrystalline silicon carbide which can be manufactured in a variety of shapes with good engineering properties (11). It was provided in the form of an extruded rod having a circular cross-section of 3 mm by the UKAEA, Springfields. It contains grains of α and β phases and free silicon, which makes it fully dense. Qualitative assessment of the relative proportions was in rough agreement with the detailed results of Sawyer and Page(12) on a similar rod; viz. 12% Si, 35% β and 53% α (of various polytypes). The free silicon may well prevent eventual usage of this material in reactor systems, but the presence of the various phases makes it a suitable choice for laboratory study.

All samples were prepared for examination in the tem prior to light-ion bombardment. This was achieved by cutting discs approximately 150-250 μm thick using a diamond wheel and mounting the discs with Durofix onto a steel plate. The discs were polished first on various SiC papers up to 600 mesh and then on 6μm down to 0.25μm diamond cloths. The discs were removed, remounted and polished on the reverse side to a final thickness of about 100 μm. The final thinning was carried out with an Ion Tech B304W Microlap ion-beam thinner using 6kV argon ions at 40 μA per ion source and an incidence angle of $10\text{-}15^{\circ}$ at perforation. Samples were injected in the HIA with either 40 or 100 keV $^4He^+$ ions at doses between 0.5 - 5 x 10^{18} cm^{-2} and temperatures of either 20° or $700^{\circ}C$.

The discs were examined before and after irradiation in the electron-transmission mode using either a Philips 400T at 100 kV or a JEOL 200B operating at 200 kV. Surface examination was undertaken in the 200B using the scanning mode and secondary-electron detector: this provides a means of correlating surface topography with underlying microstructural features. The research is still in progress, and preliminary observations are outlined here.

A typical observation of the unirradiated surface is shown in fig. 4. It can be seen that

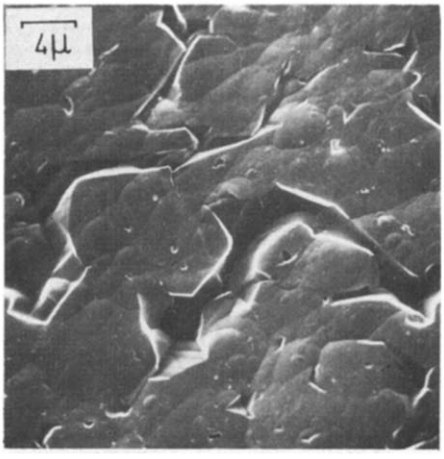

Figure 4: Secondary-electron image of the surface of an ion-thinned sample of 'Refel'.

the ion-beam thinning produces an uneven surface and the silicon grains are preferentially eroded leaving irregular cavities between the silicon carbide grains. In normal operation in the 200B, the specimen is tilted through 35° for secondary-electron imaging, a geometry in which these 50 eV electrons are most efficiently collected. However, by varying the geometry and/or operating conditions, i.e spot size, contrast, etc., additional contrast can be obtained in the image, as typified by fig. 5. This is the 'impurity-sensitive' contrast first reported by Sawyer and Page(12) using a secondary detector in an sem, and explained by them as variation in the secondary-electron coefficient

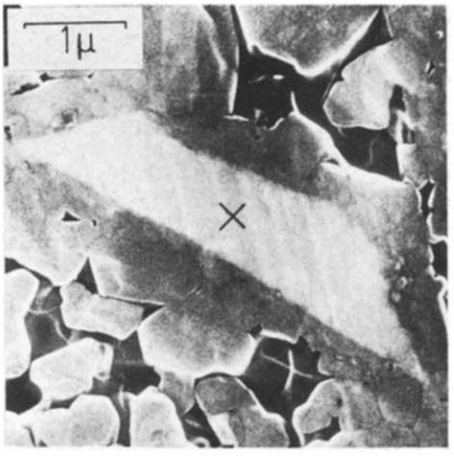

Figure 5: Secondary-electron image with impurity-sensitive contrast of ion-thinned surface.

due to the presence of trace impurities. It enables the original SiC grains, such as that labelled X in the figure, to be distinguished from the material produced in the reaction process.

From secondary-electron examination of the helium-injected surface, the irradiation at 20°C does not affect the topography in a marked way for doses up to the maximum studied (5 x 10^{18} cm^{-2}). (A few samples have been irradiated with 100 keV ions with a similar result.) There is a tendency for angular features to become rounded, due perhaps to sputtering, and evidence of intergranular and transgranular cracking is observed. Features with the appearance of shallow domes are found, but they also occur on unirradiated surfaces (see fig. 4) and are not, therefore, gas-filled blisters. They are mainly a product of sputtering by argon ions in the ion-beam thinner and simply denote variations in thickness, as has been demonstrated by comparing secondary electron-tem pairs of the same area (13). One effect of the helium ions, however, is to prevent the observation under any conditions of impurity-sensitive contrast on the irradiated side of the specimen, indicating that the secondary-electron coefficient is made uniform over the surface.

For a target temperature of 700°C, the irradiation again destroys the impurity contrast and, in addition, changes the surface morphology. A typical secondary-electron image for a dose of 5 x 10^{17} cm^{-2} at 40 keV is shown in fig. 6. This irradiated surface has flaked, and from the edges of the flaked areas, it can be seen that the flake thickness is approximately 0.2-0.3 μm, which is the most probable range of the ions. Increasing the dose to 5 x 10^{18} cm^{-2} increased the fraction of flaked surface, and in some regions it appeared that multiple flaking had occurred.

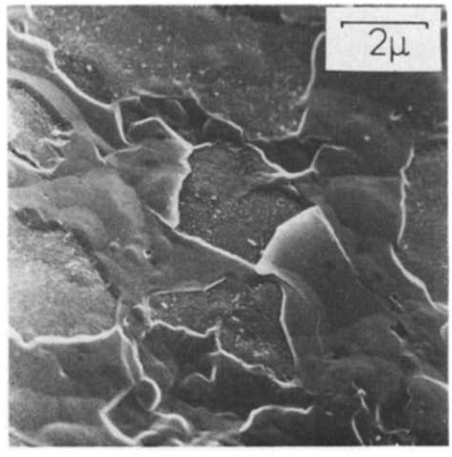

Figure 6: Surface sample injected at 700°C with 40 keV helium ions to a dose of 5 x 10^{17} cm^{-2}.

In the transmission-electron mode, all samples were found to have a thin layer of amorphous material on the surface before irradiation with helium ions. The projected width of the layer at the foil edge is typically a few tens of nm, suggesting that its thickness is just a few nm. It is believed to result from displacement damage within the range of the argon ions used for thinning and will be discussed in more detail elsewhere(13).

After irradiation with 40 keV ions to the highest dose (5 x 10^{18} cm^{-2}) at 20°C, many of the electron-transparent grains are found to be amorphous, whilst some remain crystalline and others are partially disordered. Two such areas and their diffraction patterns are shown in fig. 7. The two sorts of grain are in roughly

Figure 7: Crystalline and disordered regions in a sample at 20°C bombarded with 40 keV ions to a dose of 5 x 10^{18} cm^{-2}.

equal proportion. Within the crystalline regions, the defects observed - dislocations and stacking faults - tend to be less numerous than those seen in unirradiated samples. In a few areas, contrast from defects distributed on a very fine scale has been seen, but we are not as yet confident that they are a product of the helium irradiation. In a sample injected with 100 keV ions, no completely crystalline grains were found, although many had crystalline areas or contained impurity particles which remained crystalline. For specimens injected to the smaller dose of 5×10^{17} cm^{-2}, 40 keV ions produced no amorphous grains, whereas 100 keV ions created a mixture of amorphous and crystalline regions in approximately the same proportion as at the higher dose. Only 40 keV ions have been injected at 700°C, but even at the highest dose of 5×10^{18} cm^{-2}, the irradiation does not create amorphous grains. (The amorphous surface layer produced by thinning does persist, however.) At these temperatures, the ions produce small defects observable as either black-white dots or, in some areas, dislocation loops, see fig. 8. This displacement-induced

Figure 8: Defects in a sample injected at 700°C with 40 keV ions to a dose of 5×10^{17} cm^{-2}.

damage is believed to be interstitial loops, and details of its analysis will be reported elsewhere(13). The density of defects only increases slightly for an increase in dose from 5×10^{17} to 5×10^{18} cm^{-2}. In some regions, dense tangles of dislocations are produced by the ion bombardment and may well arise from growth and climb of the interstitial loops.

3.2 Discussion

Full discussion of these observations and results of studies using other temperatures and also deuterium ions will be the subject of a separate paper(13), but several points of importance emerge already from these preliminary findings.

Blistering, as conventionally observed in α-irradiated metals, does not occur in the α or β grains of Refel silicon carbide for doses up to 5×10^{18} cm^{-2}. Flaking is produced at 700°C, but without the formation of well-defined domes. This does not preclude the possibility that the surface is raised prior to flaking, and may reflect the lack of plasticity in silicon carbide as compared to metals. The correlation between flake thickness and depth of ion penetration leaves little doubt that the flaking is gas-induced, and the appearance of the flaked surface suggests that it may be associated with bubble formation, but we have not detected bubbles in the elctron-transparent regions.

The observation of resolvable displacement damage at the high temperature is consistent with the hvem studies of Hudson and Sheldon(14) on β-phase pyrolytic silicon carbide. They found no discrete damage for electron doses equivalent to 3 dpa at 20°C, but contrast from defects was clearly resolved for displacement values less than one half of this at 617°C. By comparison, the surface dpa values for the 40 keV helium ions employed here are between 1 and 10 for the two extremes of dose used. (These values assume a displacement energy of 106 eV for both carbon and silicon(14), which is higher than the estimate of Hart et al. (15)).

Helium-ion bombardment leaves silicon carbide in an amorphous state at 20°, but not at 700°C. This is consistent with the evidence obtained by Wright et al. (5) from Raman scattering on deuterium- and helium-bombarded material using 10 keV ions at room temperature, and with the disorder inferred by Hart et al. (15) from the back-scattering of high-energy helium and hydrogen ions from silicon carbide bombarded at 23°C with 30 and 40 keV nitrogen and antimony ions. The latter authors observed that some disorder annealed at 500°C and heavily-disordered regions annealed at 750°C. This presumably coincides with the onset of defect mobility, and is consistent with the effects seen here and the persistence up to 700°C of the layer produced by ion-thinning. Significantly, Hudson and Sheldon(14) found no loss of crystallinity under high-energy electron irradiation, which suggests that the production of amorphous material requires multiple displacement events (cascades) at high rates rather than single displacements. The modification to the band structure, as revealed by the secondary-electron contrast, is, as expected, at a much greater depth than that associated with the 6 keV argon ions, which do not destroy the impurity-sensitive contrast.

Flaking of the surface does not occur at 20°C, even at doses as large as 5×10^{18} cm^{-2}. It is probable that the observation of flaking and crystallinity at high temperatures is not mere coincidence, and that the deposition of helium atoms in a material which is being completely disordered by displacement events does not produce flaking. Two factors may lead to this

stability. First, the concentration of deposited gas will not be as strongly peaked in amorphous material, due to the absence of lattice channelling, and, second, the presence of uncollapsed cascades and disorder throughout the ion range may provide either suitable sites for the implanted atoms or easy paths for diffusion to the surface. If the amorphous material is produced by the mechanism suggested, a surface uplifting should occur whether the bombarding ion is gaseous or not.

Finally, the two sets of experiments described here show how clearly ceramics can differ in their behaviour from metals and each other. This emphasizes the important role materials research and its associated techniques must play in the development of fusion reactor systems.

ACKNOWLEDGEMENTS

This research has been supported by the SRC and the UKAEA. The assistance of R.Copp and R.W. Devenish is gratefully acknowledged.

REFERENCES

1. Das, S.K. and Kaminsky, M., Advan. Chem. Ser. 158 (1976) 112.

2. Evans, J.H., N. Nucl. Mater. 76/77 (1978) 228.

3. Rovner, L.H. and Hopkins, G., Nucl. Technol. 29 (1976) 274.

4. Bacon, D.J. and Rao, A.S., J. Nucl. Mater. 91 (1980) 178.

5. Wright, R.B., Varma, R. and Gruen, D.M., J. Nucl. Mater. 63 (1976) 415.

6. Smith, J.N., Meyer, C.H., Layton, J.K., Hopkins, G.R. and Rovner, L.H., J. Nucl. Mater. 63 (1976)392.

7. Behrisch, R., Bohdansky, J., Oetjen, G.H., Roth, J., Schilling, G. and Verbeek, H., J. Nucl. Mater. 60 (1976) 321.

8. Watanabe, K., Sasaki, M., Mohri, M. and Yamashina, T., J. Nucl. Mater. 76/77 (1978) 235.

9. Braganza, C., McCracken, G.M. and Erents, S.K., in: Proc. Intern. Sympos. on Plasma-Wall Interaction, Jülich (Pergamon, 1976) 257.

10. Mazey, D.J. and Barnes, R.S., in: Proc. 6th Intern. Conf. on Electron Microscopy, Kyoto, 1976, vol. 1, 365.

11. Forrest, C.W., Kennedy, P. and Shennan, J.V., in Special Ceramics 5, (Brit. Ceram. Res. Assoctn., 1972) 99.

12. Sawyer, G.R. and Page, T.F., J. Mater. Sci. 13 (1978) 885.

13. Dümler, I. and Bacon, D.J., in preparation.

14. Hudson, B. and Sheldon, B.E., Harwell Report: AERE-R7278 (1972).

15. Hart, R.R., Dunlop, H.L. and Marsh, O.J., in Radiation Effects in Semiconductors, (eds.) Corbett, J.W. and Watkins, G.D. (Gordon and Breach, 1971) 405.